RSC Advances

PAPER

View Article Online
View Journal | View Issue

Cite this: *RSC Adv.*, 2015, **5**, 50118

Amphiphilic quasi-block copolymers and their self-assembled nanoparticles *via* thermally induced interfacial absorption in miniemulsion polymerization†

Xianbo Xu, Guorong Shan* and Pengju Pan

A facile and nontoxic strategy for the preparation of amphiphilic quasi-block copolymers and nanoparticles has been developed utilizing miniemulsion polymerization. By volume phase transition behavior of poly(*N*-isopropyl acrylamide) (PNIPAM) and thermally induced interfacial absorption, amphiphilic copolymer was generated, which can self-assemble into core–shell nanoparticles *in situ*. Stearyl methacrylate (SMA) was used as hydrophobic monomer and to form crystalline core, because it has pendent long alkyl side chain and can form crystalline domain to synthesize comb-like polymers. A volatile organic cosolvent was used to enhance the formation process and particles size, and the formation mechanism was investigated. Impacts of cosolvent concentration, monomer feed ratio and polymerization temperature on the morphology and thermal characteristics of particles were studied by DLS, TEM and DSC. ^{1}H NMR, ^{13}C NMR and GPC were carried out to analyze the chemical structure and composition of copolymers. The triads sequence and average block length are analyzed to determine the sequence distribution of copolymers. Volume phase transition temperature (VPTT) of PNIPAM copolymer was first increased to nearly 40 °C with hydrophobic monomer rather than hydrophilic monomer. In addition, hydrophilic property of copolymer and the drug release behavior were studied to understand further applications. These amphiphilic quasi-block copolymers show great potential in the controlled delivery system for drugs.

Received 20th April 2015
Accepted 1st June 2015

DOI: 10.1039/c5ra07087b

www.rsc.org/advances

Introduction

Amphiphilic block copolymers are obtained by polymerization of two or more monomers, typically one hydrophobic and one hydrophilic, hence to get macromolecules composed of moieties that have different affinities for an aqueous solvent and self-assembled in selective solvents to form aggregates.[1,2] Amphiphilic core–shell polymeric particles that consist of hydrophobic cores coated with hydrophilic shells have attracted considerable attention because of their wide application in gene and drug delivery, diagnostic test, biochemical separation and modern material science.[3–5] Miniemulsion polymerization of hydrophobic and hydrophilic monomers is a direct method for preparing such polymeric particles. This copolymerization of monomers with very different water solubilities has long been an active field of research and a big challenge, because hydrophilic monomer resides almost in the aqueous phase while hydrophobic monomer resides almost always in the organic phase.[6] Although the controlled free-radical polymerization techniques such as nitroxide-mediated polymerization, atom transfer radical polymerization, and reversible addition–fragmentation chain transfer (RAFT) polymerization have been used for the preparation of amphiphilic core–shell particles, they are multi-step syntheses of polymer, containing control free-radical moiety with potentially toxic and needing tedious purification steps. This would greatly limit their applications in biology and medicine.[7] However, most amphiphilic copolymer studies were limited by the incorporation of hydrophilic monomer into the copolymer, which needs further research to work out.[6,8]

Thermo-sensitive polymer poly(*N*-isopropylacrylamide) (PNIPAM) possesses a volume phase transition temperature (VPTT) of about 32 °C, which is close to the temperature of human body.[9] Due to its ability to shrink at temperatures above VPTT and to swell below it, PNIPAM-based copolymers can be used for controlling of drug release by simple temperature changes.[10,11] For the purposes of drug targeting, researchers usually increase this phase transition temperature to about 40 °C by introducing a hydrophilic comonomer, which however, leads to a decrease of temperature sensitivity of copolymer, as well as the load ability of lipophilic drugs.[12] There is rarely report on introducing hydrophobic monomer solely and increasing VPTT at same time. Stearyl methacrylate (SMA) is quite hydrophobic due to the pendent long alkyl side chain. As

State Key Laboratory of Chemical Engineering, Department of Chemical and Biological Engineering, Zhejiang University, 38 Zheda Road, Hangzhou 310027, China. E-mail: shangr@zju.edu.cn; Tel: +86-571-87951334

† Electronic supplementary information (ESI) available. See DOI: 10.1039/c5ra07087b

SMA could form crystalline domain to synthesize comb-like polymers, its interesting solution behaviors had attracted a lot of attentions.[13–15]

In this work, PNIPAM is used to conduct miniemulsion polymerization of hydrophobic and hydrophilic monomers, in a simple and direct way to form amphiphilic core–shell polymeric particles. The solubility and thermosensitivity of PNIPAM are particularly utilized to produce interfacial adsorption and incorporation into oil phase. On the other hand, the VPTT of PNIPAM copolymer was just increased to nearly 40 °C without hydrophilic monomer. SMA was used to form the hydrophobic and crystalline core for loading and retaining drugs. Variables influence the morphology, thermal characteristics and hydrophilic property of copolymer nanoparticles were investigated, and the possible mechanism involved was discussed.

Experimental

Materials

Stearyl methacrylate (SMA, 95.5%, TCI) and *N*-isopropylacrylamide (NIPAM, Acros Organics) were purified by recrystallization in *n*-hexane and then dried in a vacuum oven at room temperature. Potassium persulfate (KPS, Acros organics) was used as initiator. Sodium dodecyl sulfate (SDS, 99%, Acros Organics), ibuprofen (98%, J & K), *n*-hexane and other reagents were of analytical grade and used as received. Deionized water was applied for all of the polymerization and treatment process.

Synthesis of quasi-block polymer nanoparticles

Quasi-block polymer nanoparticles were prepared by miniemulsion polymerization. The typical procedure was as follows. Monomers SMA and NIPAM were mixed in *n*-hexane to obtain oil phase. This oil phase was stirred and dissolved at 50 °C, and then added to the aqueous solution containing surfactant SDS. The miniemulsion was prepared by ultrasonifying the mixture for 20 min using a pulsed sequence (10 s sonication followed by 5 s break) with a 560 W duty cycle (SCIENTZ, JY92) under magnetic agitation in an ice bath. The polymerization was carried out in a jacketed reactor and under nitrogen atmosphere. Temperature was raised to 70 °C, and an aqueous solution of KPS was fed into reactor to start polymerization. The polymerization was continued for 6 h under stirring at 300 rpm, and then the miniemulsion was cooled to room temperature. The purified PNIPAM/PSMA copolymer was obtained as follows: copolymer solution was subjected to centrifugation at 10 000 rpm min^{-1} for 10 min to get precipitation and re-dispersed in deionized water; this centrifugation was carried out three times to remove PNIPAM homopolymer and NIPAM monomer; precipitation was dissolved in THF and then precipitated in toluene to remove PSMA homopolymer and SMA monomer; eventual precipitation was dried in a vacuum oven overnight. The proportions of reagents and detailed conditions in nanoparticle syntheses are given in Table 1.

Characterization

The particle size and size distributions (PDI) were measured by dynamic light scattering (DLS, Zetasizer 3000 HSA, Malvern) at different temperatures. PDI is a dimensionless index that describes the distribution of particle size and it ranges from 0 (monodisperse) to 1 (polydisperse). The nanoparticles were dispersed in deionized water before analysis. Five repeated measurements were performed for each sample and the averaged result was used.

Molecular weight and molecular weight distribution were determined on a Waters Alliance e2695 gel permeation chromatograph (GPC) equipped with a Waters Styragel column, a dual-wavelength ultraviolet-visible detector and a differential refraction detector (Waters 2414). THF was employed as the eluent at a flow rate of 1.0 mL min^{-1}. Molecular weights of samples were determined with the calibration of polystyrene standards.

Table 1 Composition of the miniemulsions and properties of copolymer nanoparticles[f]

Sample	Molar ratio of SMA to total monomer (%)	Polymerization temperature (°C)	*n*-hexane (g)	M_n[a] (g mol^{-1})	M_w/M_n[b]	d_z[c] (nm) 25 °C	d_z[c] (nm) 50 °C	Swelling ratio[d]	PDI[e] 25/50 °C
NP21	33	70	5.0	301 500	1.78	81.6 ± 0.9	64.4 ± 0.2	2.03	0.216/0.185
NP11	50	70	5.0	401 200	1.77	82.5 ± 1.1	74.7 ± 0.8	1.35	0.171/0.114
NP12	67	70	5.0	452 200	2.52	92.7 ± 0.5	90.1 ± 0.7	1.09	0.322/0.169
NP13	75	70	5.0	509 800	2.85	99.5 ± 0.6	103.1 ± 1.1	0.90	0.334/0.184
NP14	80	70	5.0	515 500	3.02	106.1 ± 0.7	113.0 ± 0.9	0.83	0.338/0.223
NP50	50	50	5.0	451 520	2.27	107.2 ± 1.2	99.6 ± 0.7	1.25	0.238/0.142
NP60	50	60	5.0	416 800	1.85	94.7 ± 0.9	88.4 ± 0.2	1.23	0.227/0.205
NP70A	50	70	/	360 200	2.03	170.4 ± 1.6	158.4 ± 1.2	1.24	0.241/0.177
NP70B	50	70	8.0	405 100	1.79	73.4 ± 0.9	63.8 ± 0.7	1.52	0.174/0.117
NP80	50	80	5.0	375 740	1.72	85.5 ± 1.0	83.1 ± 0.8	1.09	0.269/0.226
PSMA	100	70	5.0	540 770	2.76	103.3 ± 1.4	104.9 ± 1.2	0.95	0.195/0.143

[a] Determined by GPC with THF as the eluent. [b] M_w/M_n represents the polydispersity index of the molecular weight obtained by GPC. [c] The diameter was measured by DLS (5 mg mL^{-1}). [d] Swelling ratio was calculated with $SR = \frac{V_{50\,°C}}{V_{25\,°C}} \times 100\%$. [e] PDI represents polydispersity index obtained by DLS. [f] The usages of KPS, SDS, and total monomer are kept as 0.02 g, 0.12 g, and 20 mmol, respectively.

The oil–water partition coefficients of NIPAM and conversion of samples were determined by gas chromatography (GC, Agilent 6890 equipped with INNOWAX capillary column). THF was used as an internal standard. Samples were subjected to GC analysis by internal standard method utilizing a relative mass correction factor for peak areas.

Chemical structures of copolymers were studied by ^{1}H NMR and ^{13}C NMR on an Agilent DD2-600 nuclear magnetic resonance (NMR) instrument using $CDCl_3$ as solvent and tetramethylsilane (TMS) as the internal standard.

Transmission electron microscopy (TEM) measurements were performed on a JEOL JSM-1230EXT2 Microscope. Diluted dispersions in water were held at different temperature for 2 h, deposited on 400-mesh carbon-coated copper grid, and dried at different temperature for analysis.

Differential scanning calorimetry (TA DSC Q200) was used to measure the volume phase transition temperature of nanoparticles. Samples, at a concentration of 5 wt%, were heated in the range from 10 to 60 °C at a heating rate of 2 °C min^{-1}. Sample analysis was performed in hermetically sealed alumina pans and under a nitrogen flow of 60 mL min^{-1}. VPTT was designated by the maximum temperature of endothermic peak. The scans were performed in triplicates.

Contact angle was measured with a sessile drop configuration on a contact angle meter dataphysics OCA20 (Data Physics Instruments GmbH, Germany). Copolymer solutions (10 mg mL^{-1}) were spin-coated on a glass slide and dried in different conditions. A droplet of 3 μL water was deposited on the surface of copolymer film and the shape of droplet was recorded immediately to determine the contact angle. The measurement was repeated 4 times at different positions of films.

Sample NP11 was chosen for study of drug delivery. Ibuprofen, a typical hydrophobic drug, was used as a model drug and incorporated into nanoparticles. Copolymer nanoparticles were ultrasonic dispersed in phosphate buffered solution (PBS, pH = 7.4) of ibuprofen with a concentration of 2 mg mL^{-1}. After continuously stirring for 6 h at desired temperature, the nanoparticles were loaded with ibuprofen by diffusion and adsorption and then centrifuged at 10 000 rpm min^{-1} for 10 min to get the drug loaded nanoparticles. This centrifugation was carried out three times to remove the excess drug and the supernatant was analyzed using ultraviolet-visible spectrophotometer (SHIMADZU UV-1800). The precipitate was washed with deionized water and then freeze-dried. The *in vitro* drug release behaviors were determined using a dialysis technique. Drug-loaded nanoparticles (50 mg) were dispersed in 20 mL PBS, and introduced into a dialysis tube (Spectra/Por®2, 12 000 to 14 000 molecular-weight cut-off, Spectrum Medical Industries, Inc., CA, USA) immersed into 500 mL PBS at the desired temperature. At each time interval, 5 mL released solvent was taken out for UV spectrophotometer measuring the maximum wavelength (263 nm) absorbance of ibuprofen. Withdrawn solvent was replaced with the same volume of fresh PBS. Accumulated release rate (R) was calculated as follows:

$$R = \frac{VC_i + v\sum C_{(i-1)}}{m} \times 100\% \quad (1)$$

where V is the total volume of dialysate and v is sampling volume. C_i is the measured drug molality at each time and m is the total mass of loaded drug. Drug release experiments were conducted for about 24 h until the concentration stabilized. Using the absorbance values obtained from the spectrophotometer, the amount of drug released was determined as a function of time.

Results and discussion

Structure characteristics of copolymers

^{1}H, ^{13}C NMR and GPC measurements were carried out to confirm the chemical structure, composition, and molecular weights of copolymers. ^{1}H NMR spectra of PSMA homopolymer and PNIPAM/PSMA quasi-block copolymer (Fig. S1, ESI†) confirmed that SMA took part in copolymerization reaction successfully. Moreover, the composition of quasi-block copolymer can be determined from ^{13}C NMR spectrum.

^{13}C NMR spectrum of PNIPAM/PSMA quasi-block copolymer (sample NP11) is shown in Fig. 1A. The carbon of methylene group adjacent to the oxygen atom shows a chemical shift at 64 ppm (b), which exhibits a sharp peak and is not influenced by components and stereostructure. Peaks at 35–48 (c) and 13–32 ppm (d) are attributed to carbon in the backbone and carbon of methylene and methyl groups in the side chains, respectively. The spectra are quite complex because different stereosequences of triads and stereostructure lead to the splittings and shifts of these signals. However, peaks of the carbonyl carbon between 174 and 178 ppm (a) are relatively simple and also sensitive to substituent differences in microstructural environments, and hence they are selected for further analysis. The magnified spectra show multiple peaks (at least eight peaks) because of different sequence distributions and conformations. The analysis and assignment of the resonance pattern of carbonyl carbon atoms of SMA (S) and NIPAM (N) centered triads sequence is given in Table 2. Peaks 1, 2, and 3 in lower field of carbonyl signal correspond to SMA triads (SSS), and the three splitting peaks and peak shifting are due to the isotactic or syndiotactic type of stereoregularity in SMA. Peak 8 in high field corresponds to NIPAM triads (NNN).[16,17] In particular, the spectra shows additional splittings, and new peaks (4, 5, 6, and 7) are clearly observed. As one SMA monomeric unit in SSS

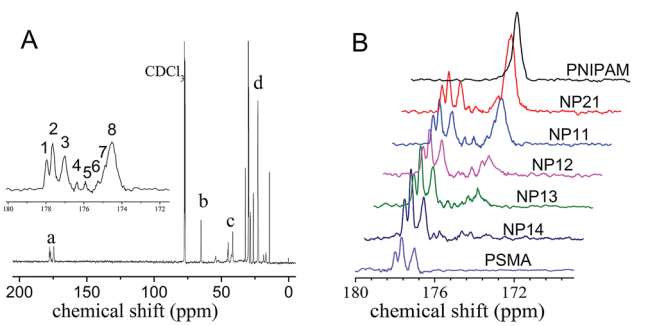

Fig. 1 ^{13}C NMR spectra of copolymer (A) sample NP11; (B) comparison of copolymers and homopolymers in the carbonyl carbon region.

Table 2 Assignment of resonance peaks of carbonyl carbon atoms of S and N centered sequence (sample NP11)

Spectral signal	Chemical shift (ppm)	Triad sequence
1	177.96	SSS
2	177.65	SSS
3	177.01	SSS
4	176.36	NSS, SSN
5	175.92	SNS
6	175.26	NSN
7	174.86	NNS, SNN
8	174.52	NNN

triads is replaced by NIPAM, the carbonyl signal of copolymer shifts to higher field. The assignment is shown in Table 2. Comparison of copolymers and homopolymers in carbonyl carbon region (Fig. 1B) shows additional splittings evidently and the intensity of spectra reduced with the NIPAM content decreasing. The peak intensity reflects the relative contents of copolymer composition. ^{13}C NMR spectra are gated-decoupled and can therefore be accurately integrated.[18]

The average sequence length, alternating degree (χ), degree of randomness (R) and D value in Table 3 are calculated from ^{13}C NMR Spectra according to the analysis of triad sequences.[16–19] Alternating degree describes the molar fractions of alternating sequence in total sequence. The D value is used to characterize the dyad sequence distribution of polymers. R and D are represented by

$$R = (F_{NS}/2)/F_N + (F_{NS}/2)/F_S \quad (2)$$

$$D = F_{NN}F_{SS}/F_{NS}F_{NS} \quad (3)$$

where F_N and F_S are the relative molar fractions of NIPAM and SMA, respectively; F_{NS}, F_{NN}, and F_{SS} indicate the relative molar fractions of corresponding dyad sequences. The triad fractions determined from carbonyl carbon resonances can be used to calculate the dyad fraction distribution. $R > 1$ indicate that the units have a more alternating distribution. When $R < 1$, the distribution of units tend to be homogeneous and thus the copolymer exhibits a block character. A random copolymer has a D value of 1.0, while block and alternative copolymers have a D value larger and lower than 1, respectively.[20] Copolymer composition clearly affects the average block length. The average block length of NIPAM strongly decreases as its content reduces, and the average block length of SMA is correspondingly increased. When the content of one monomer is relatively very low, it will be very hard to achieve long homologous block lengths. On the other hand, when the compositions are balanced against each other, larger block lengths can be obtained. As seen from the value of alternating degree (χ), copolymer has a block character. The value of χ is decreased with NIPAM content, because in this case less NIPAM permeates to oil phase to initiate polymerization of SMA, leading to a decrease of alternating degree. All of the D values are much bigger than 1, indicating that sequence distribution of copolymers is a large possibility to be block. And the randomness degree R indicates that sequence distribution is more likely to be block too ($R < 1$), in accordance with the result of D values. While, R value is increased with NIPAM content reduces, demonstrating that the block copolymer is harder to be obtained with less NIPAM permeating to oil-phase. From these results, it can be concluded that this thermally induced mini-emulsion copolymerization provide a practical method for the preparation of block copolymer.

The molecular weight (M_n) changes with different polymerization temperature as well as feed ratio of SMA (Fig. S2 and S3, ESI†). The GPC traces showed that each of these samples had a single peak, and that the molecular weight was decreased with NIPAM content, and also decreased with higher reaction temperature due to the faster polymerization and termination rate. At higher temperature, the oligomers, formed by NIPAM in water, would dissolve in oil phase with lower polymerization degree and can fast initiate polymerization of hydrophobic monomer.[21] Thus, the molecular weight was decreased and the content of SMA in copolymers was relatively decreased due to faster polymerization and termination rate at higher temperatures. However, the feed ratio of SMA had a bigger influence on M_n. M_n values increased linearly with SMA content, and nanoparticle size and PDI were increased accordingly (Table 1). As the proportion of NIPAM was quite low, PNIPAM oligomers were not enough to coat oil droplets, and thus led to bigger particle size and broader distribution. Moreover, as PNIPAM moiety decreased and particle size increased, the thermo-sensitivity changes of nanoparticles were less pronounced. This could be attributed that PNIPAM oligomers not only acted as a thermo-sensitivity moiety copolymerized with a hydrophobic monomer, but also as a stabilizer to stabilize the resultant particles during polymerization.[22,23] Thus, stable

Table 3 Molar composition, average sequence lengths and alternate degree calculated from ^{13}C NMR spectra

		Average sequence lengths				
Sample	Molar composition (F_N/F_S)	L_N	L_S	Alternating degree (χ)	Degree of randomness (R)	D value
NP21	1.89	29.49	5.61	0.090	0.21	131.26
NP11	0.90	9.16	16.84	0.083	0.18	163.04
NP12	0.37	6.43	21.13	0.078	0.21	157.43
NP13	0.26	5.39	23.52	0.075	0.26	98.78
NP14	0.083	2.32	37.23	0.072	0.53	42.63

amphiphilic core–shell particles can be produced with a smaller size and narrower size distribution.

Synthesis of quasi-block copolymers and formation of nanoparticles

Nanoparticle with core–shell structure was synthesized as amphiphilic quasi-block copolymer consisting of a thermoresponsive PNIPAM moiety and a hydrophobic moiety. The water solubility of the thermoresponsive moiety can be altered by changing temperature, which is the key point for synthesis of quasi-block copolymer. Fig. 2 illustrates the formation and structure characteristics of amphiphilic core–shell nanoparticles. PNIPAM exhibits a VPTT at which the polymer solution undergoes a phase transition from a soluble to an insoluble state when temperature is raised. After initiating polymerization, NIPAM in water will form oligomers, followed by the attachment of sulfate radical anion to the end chain. As its solubility in water changed at the temperature above VPTT, PNIPAM oligomers were tended to be adsorbed to the surface of oil phase and then initiated polymerization of hydrophobic monomer, resulting in the formation of a block copolymer. The amphiphilic copolymer generated can self-assemble into particles *in situ*, especially in the environment of volatile organic cosolvent, which is promoting the copolymerization with hydrophobic monomer and helping forming nanoparticles.

It should be emphasized that, we all know the water solubility of PNIPAM sharply changes with temperature. However, besides that, NIPAM monomer has a small partition in oil phase. The oil–water partition coefficient of NIPAM in *n*-hexane and SMA shows that NIPAM is slightly soluble in oil phase and its solubility in oil droplets of *n*-hexane and SMA increases with temperature obviously (Table S1, ESI†). This indicates that, when forming miniemulsion, a small amount of NIPAM in oil droplets would copolymerize with SMA to form the hydrophobic moiety. Increasing temperature would increase the incorporation of hydrophilic monomer into copolymer; this will lead to the copolymerization of hydrophobic and hydrophilic monomers inside the droplets and the formation of amphiphilic copolymers. The conversion *vs.* time curves for miniemulsion polymerizations of SMA were plotted in Fig. 3. Polymerization rate of NIPAM was faster than SMA in first 20 min, then the polymerization rate of NIPAM decreased and SMA increased. After about 60 min, the conversion of SMA kept almost constant, while the conversion of NIPAM increased gradually. However, SMA had a slow polymerization rate and low conversion in the absence of NIPAM. Because the polymerization rate and conversion of SMA were significantly promoted by NIPAM, PNIPAM oligomers were proved to have effective penetration into hydrophobic monomer droplets with increasing temperature. It is considered that the majority of SMA was initiated by PNIPAM oligomers.

As amphiphilic quasi-copolymer generated *in situ* and self-assemble into particles, the volatile organic cosolvent shows great impact on nanoparticle size and morphology. With the increase of *n*-hexane content (Table 1, samples NP70A, NP11 and NP70B), nanoparticle sizes were decreased from 170.4 to 73.4 nm and polydispersity became smaller. The volatile solvent *n*-hexane is evaporated during polymerization, either directly from oil phase or by dissolution into surrounding aqueous phase and evaporated thereafter. Therefore, the droplets size is decreased and the concentration of quasi-block copolymer in droplets is increased.[24] Thus, some large droplets would suffer

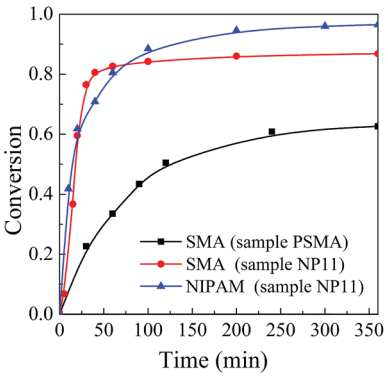

Fig. 3 Conversions of SMA and NIPAM in miniemulsion copolymerization (Table 1, PSMA and NP11).

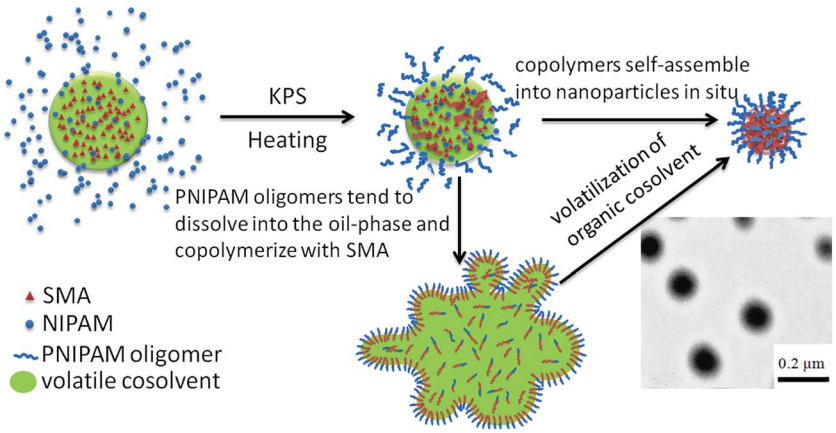

Fig. 2 Formation mechanism of amphiphilic core–shell particle *via* thermally induced interfacial polymerization.

with rough interface between organic solvent and water, which tended to dissolve into aqueous phase and form smaller micelles. What is more, *n*-hexane suppressed the Ostwald ripening between the monomer droplets by evaporating and reducing the interfacial tension. The particles sizes varied with different *n*-hexane content and reaction time were shown in ESI Fig. S4.† The increase in the amount of cosolvent would cause a decrease in the size of monomer droplets and prevent larger particles growing, thus leading to a decrease in the size of the resulting nanoparticles. Consequently, the most common morphologies were the core–shell structure nanoparticles (TEM image in Fig. 2) in the range of 70 to 120 nm in diameter.

Thermal characteristics and nanoparticle morphology

PNIPAM homopolymer is known to exhibit a VPTT at 32 °C.[9] DSC curves of quasi-block copolymer nanoparticles are displayed in Fig. 4. These DSC results show higher VPTT values of 35–40 °C. This temperature is suitable for controlled drug release. The phase transition temperature of PNIPAM is generally increased by introducing a hydrophilic comonomer and decreased by introducing a hydrophobic comonomer because the hydration of PNIPAM chain could be strengthened or weakened by the comonomer.[25] However, Nakayama *et al.*[10] indicated that the hydrophobic chain did not directly influence the transition temperature of hydrophilic chain in the block copolymers. Therefore, this result also demonstrated that quasi-block copolymer was successfully prepared because the VPTT did not decrease. It was considered to be increased by the terminal hydrophilic sulfate radical group and decreased by the presence of hydrophobic PSMA moiety.[26,27] The crystalline property of PSMA was thought to influence the VPTT of copolymers as well. The VPTT of PNIPAM/PSMA quasi-block copolymer was slightly increased with higher content of SMA or higher reaction temperature. Melting temperature of PSMA was about 42.6 °C, higher than the VPTT of PNIPAM (32 °C). Because the melting temperature of PSMA and VPTT of PNIPAA are in the similar temperature range, the endothermic peaks of copolymers in DSC would include both contributions of melting of PSMA unit and volume phase transition of PNIPAM unit. VPTT of PNIPAM/PSMA quasi-block copolymer would increase by the terminal hydrophilic sulfate radical group and decrease by the presence of hydrophobic PSMA moiety. It cannot draw a clear conclusion on the changing trend of copolymer VPTT with NIPAM content on basis of the DSC results. The change of DLS size with temperature (Fig. S5, ESI†) showed that particle sizes of copolymers with high NIPAM content suddenly decreased with temperature increasing. However, the change of DLS size is not very obvious upon heating and the transition temperature cannot be precisely evaluated from the DLS results, especially for the samples with higher SMA contents.

The pendent long alkyl side chain of SMA can form crystalline domain, making polymer phase transition. The crystalline domain has certain mechanical strength, hardness and lower permeability.[28,29] However, it will turn to an amorphous state and show favorable permeability above the melting temperature. Block copolymerization decrease the crystallinity of PSMA and nano-sized particles make PSMA not forming big size crystal. These make the melting temperature of PSMA moiety in PNIPAM/PSMA copolymer decreased. Consequently, their DSC peaks are going to be a similar temperature range and overlapped. Because the melting temperature of PSMA and VPTT of PNIPAA are in the similar temperature range, the transition of nanoparticles is particularly interesting. PNIPAM moiety will shrink and PSMA moiety is swelling and amorphous upon heating. Nevertheless, when cooling, the PNIPAM moiety is swelling and could dissolve in water and PSMA moiety crystallized into ordered domain (shown in Fig. 5). The diluted dispersions of sample NP11 in water were held at specified temperature for 2 h and then deposited on 400-mesh carbon-coated copper grid and dried at specified temperature for TEM measurement. Fig. 5a should be the transition state of not fully curled up PNIPAM units and not crystallized PSMA units. With temperature increasing, the particle size is decreased from 82.5 nm (25 °C) to 74.7 nm (50 °C), and PDI also decreased from 0.171 (25 °C) to 0.114 (50 °C), which is shown in Table 1. The nanoparticles are more homogeneous at high temperature (Fig. 5b). However, PNIPAM units gradually become stretched with the temperature decreases, making nanoparticles bigger size and relatively uneven distribution (Fig. 5c). The swelling ratios were shown in Table 1. PNIPAM chains would curl up and the PSMA chains would slightly swell with temperature

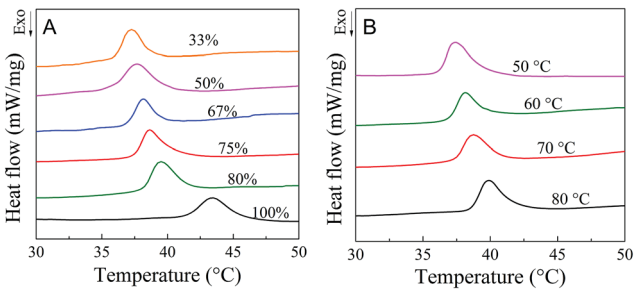

Fig. 4 DSC thermograms of copolymers with different feed ratio of SMA (A) and polymerization temperature (B).

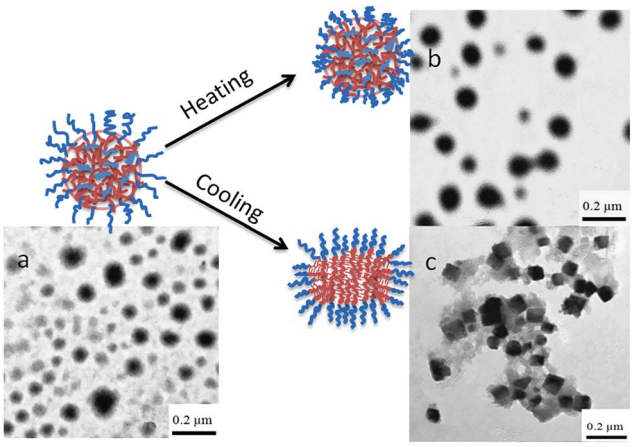

Fig. 5 Schematic model and TEM images of sample NP11 for the transition of nanoparticles at different temperatures: (a) 35 °C; (b) 50 °C; (c) 20 °C.

increasing. These opposite changes caused by rising temperature could both switch on the pathway to delivering substances in nanoparticles. However, these changes make the swelling ratio not accurately reflect the drug delivering property of nanoparticles.

Hydrophilic property

To further understand the amphiphilic quasi-block copolymer and its potential applications, the surface hydrophilic property was studied. When nanoparticles are loaded with hydrophilic or lipophilic drugs, the surface hydrophilic property is important to the release behavior for different requirements *in vivo*.[30] Copolymer films were prepared in different drying methods and the contact angle was measured as shown in Fig. 6.

Both of the drying methods and contents of SMA in copolymer show a significant influence on contact angle. The hydrophobic PSMA moiety formed core, which was surrounded by PNIPAM moiety. With the increase of PSMA content, PNIPAM moiety was not enough to cover the core and the hydrophobic moiety was exposed. The contact angle increased because PSMA moiety gradually became the major part of surface composition. When the content of SMA is over 70%, the films are hydrophobic regardless of the drying methods. However, the drying methods also could change films from hydrophilic to hydrophobic. When the film was dried in oven, PNIPAM was shrunken into coils and shown as hydrophobic. However, compared with PSMA moiety, the shrunken PNIPAM is still hydrophilic. When freeze-dried, PNIPAM was fully stretched and became the main composition in surface. As PNIPAM showed hydrophilic behavior, it would make the nanoparticles soluble in water.

Drug release behavior

The release behavior of model drug was observed at temperatures above and below the VPTT of the block copolymer in PBS at pH 7.4. The time-dependent release data are displayed in Fig. 7. As the Weibull model eqn (4) has been widely applied to release data of drug delivery systems, it is used to fit the release date.[31]

$$\text{Weibull model} \quad \ln[-\ln(1-m)] = \beta \ln(t - T_i) - \ln \alpha \qquad (4)$$

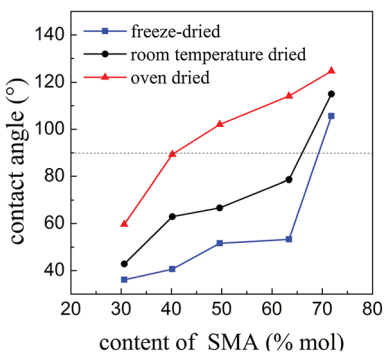

Fig. 6 Surface hydrophilic property of copolymer films with different contents of SMA and different drying methods.

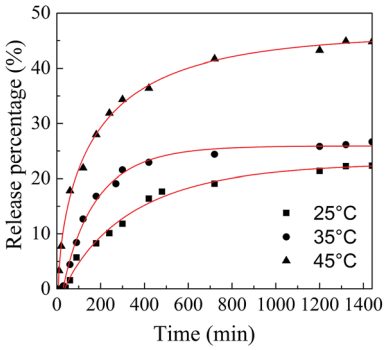

Fig. 7 Profiles of ibuprofen release from nanoparticles (sample NP11) in PBS at different temperatures.

where m is the accumulated fraction of the drug; β is the shape parameter; α is the scale parameter; T_i is the location parameter.

The linearity of the Weibull plots are shown in Fig. 7. The parameters calculated by the model and the determination coefficients (R^2) obtained are summarized in Table 4.

The release property of ibuprofen shows the temperature has big effect on the release behavior. It was observed that, at all three temperatures, the nanoparticles continued to release the drug in 24 h, illustrating a better sustained release effect of nanoparticles. The release rate at 45 °C was much faster because of the collapse of PNIPAM chains at temperatures above VPTT, which opened more tunnels for diffusion of ibuprofen. And PSMA chains turn to an amorphous state and show favorable permeability above the melting temperature. Weibull model is well fitted for this drug release mechanisms and all the determination coefficients (R^2) are greater than 0.99. In terms of applicable parameters, described by Weibull model, the shape parameter, β, characterizes the curve as either exponential ($\beta = 1$), S-shaped with upward curvature ($\beta > 1$), or as curve with steeper initial slope than consistent with the exponential ($\beta < 1$).[32] Weibull β parameter is <1 for all release behavior (Table 4), suggesting that they are the same curve shape with steeper initial slope, and curves at 25 °C and 35 °C are much more similar. The location parameter T_i, shows the nanoparticles could delayed-release drugs and the delayed time reduced with temperature rising, from 36.46 min to 7.03 min for ibuprofen. Scale parameter (α) has a negative correlation with the diffusion coefficient, which shows the release rate at 45 °C is about four times larger than 35 °C and seven times larger than 25 °C. There are striking changes signified that the temperature could

Table 4 Parameters and determination coefficients of the Weibull model obtained for drug release from nanoparticles at different temperature

Parameters	α	β	T_i	R^2
25 °C	176.37	0.89	36.46	0.9912
35 °C	99.80	0.91	29.17	0.9938
45 °C	26.39	0.62	7.03	0.9970

control the release of ibuprofen. This drug release behaviors can be used for extended and controlled releasing of drugs.

Conclusions

A novel, nontoxic, and simple approach to synthesize amphiphilic quasi-block copolymers and nanoparticles in aqueous medium was demonstrated. This method exploited the variation of polymer upon VPTT, because its solubility and oil–water partition are all greatly changing with temperature. Rising temperature could effectively increase the incorporation of PNIPAM oligomers into oil phase and set the stage for direct copolymerization of hydrophobic and hydrophilic monomers by emulsion polymerization. The results of ^{1}H, ^{13}C NMR, DSC and TEM proved the successfully formation of block structure of copolymer. The average block length, particle size, M_n and dispersion of copolymer nanoparticles could be controlled by monomer feed ratio, cosolvent concentration and polymerization temperature. A volatile organic cosolvent can be used to adjust the formation process and particles size, and growth mechanism for this polymerization method was investigated.

The nanoparticle had a thermo-sensitivity and hydrophilic shell, and a hydrophobic and crystalline core. The VPTT of copolymer was increased to about 40 °C, which was suitable for biomedical applications. Furthermore, thermal characteristics, hydrophilic property and drug release behavior of copolymer nanoparticles were studied to show great potential in controlled delivery system of drugs.

Acknowledgements

We thank the National Natural Science Foundation of China (21176210), Outstanding Youth Foundation of Zhejiang Province (R4110199), and the Innovation Research Team of Zhejiang Province (2009R50016) for financial support.

Notes and references

1 W. Steinhauer, R. Hoogenboom, H. Keul and M. Moeller, *Macromolecules*, 2013, **46**, 1447–1460.
2 R. Vyhnalkova, A. H. E. Müller and A. Eisenberg, *Langmuir*, 2014, **30**, 5031–5040.
3 H. Ajiro, Y. Takemoto and M. Akashi, *Chem. Lett.*, 2009, **38**, 368–369.
4 Y. Gu, Y. Zhong, F. Meng, R. Cheng, C. Deng and Z. Zhong, *Biomacromolecules*, 2013, **14**, 2772–2780.
5 Z. Xing, C. Wang, J. Yan, L. Zhang, L. Li and L. Zha, *Soft Matter*, 2011, **7**, 7992–7997.
6 Y. Luo and F. J. Schork, *J. Polym. Sci., Part A: Polym. Chem.*, 2001, **39**, 2696–2709.
7 K. Ho, W. Li, C. Wong and P. Li, *Colloid Polym. Sci.*, 2010, **288**, 1503–1523.
8 R. G. Gilbert, J. F. Anstey, N. Subramaniam and M. J. Monteiro, *National Meeting of the American Chemical Society*, 1999, vol. 218, p. U401.
9 Z. Li, K. Geisel, W. Richtering and T. Ngai, *Soft Matter*, 2013, **9**, 9939–9946.
10 M. Nakayama, T. Okano, T. Miyazaki, F. Kohori, K. Sakai and M. Yokoyama, *J. Controlled Release*, 2006, **115**, 46–56.
11 X. Xu, G. Shan, Y. Shang and P. Pan, *J. Appl. Polym. Sci.*, 2014, **131**, 40589.
12 D. Kuckling, H. J. P. Adler, K. F. Arndt, L. Ling and W. D. Habicher, *Macromol. Chem. Phys.*, 2000, **201**, 273–280.
13 S. Qin, K. Matyjaszewski, H. Xu and S. S. Sheiko, *Macromolecules*, 2003, **36**, 605–612.
14 J. Zhou, L. Wang, Q. Yang, X. Dong and H. Yu, *Colloid Polym. Sci.*, 2007, **285**, 1369–1376.
15 C. Liu, P. Ni, X. Fang and X. Zhou, *Colloid Polym. Sci.*, 2009, **287**, 45–55.
16 I. Tritto, C. Marestin, L. Boggioni, L. Zetta, A. Provasoli and D. R. Ferro, *Macromolecules*, 2000, **33**, 8931–8944.
17 F. Samperi, M. S. Montaudo, C. Puglisi, S. Di Giorgi and G. Montaudo, *Macromolecules*, 2004, **37**, 6449–6459.
18 A. M. Aerdts, K. L. L. Eersels and G. Groeninckx, *Macromolecules*, 1996, **29**, 1041–1045.
19 H. Matsuda, B. Nagasaka and T. Asakura, *Polym. J.*, 2003, **35**, 740–747.
20 F. Yu, T. Dong, B. Zhu, K. Tajima, K. Yazawa and Y. Inoue, *Macromol. Biosci.*, 2007, **7**, 810–819.
21 H. Lai, Q. Chen and P. Wu, *Soft Matter*, 2013, **9**, 3985–3993.
22 Z. H. Cao, G. R. Shan, N. Sheibat-Othman, J. L. Putaux and E. Bourgeat-Lami, *J. Polym. Sci., Part A: Polym. Chem.*, 2010, **48**, 593–603.
23 S. Ma, M. Xiao and R. Wang, *Langmuir*, 2013, **29**, 16010–16017.
24 M. Su and Z. Su, *Macromolecules*, 2014, **47**, 1428–1432.
25 S. Petrusic, P. Jovancic, M. Lewandowski, S. Giraud, S. Grujic, S. Ostojic, B. Bugarski and V. Koncar, *J. Mater. Sci.*, 2013, **48**, 7935–7948.
26 Y. Xia, N. A. D. Burke and H. D. H. Stöver, *Macromolecules*, 2006, **39**, 2275–2283.
27 A. S. Hoffman, *Adv. Drug Delivery Rev.*, 2002, **54**, 3–12.
28 K. A. O'Leary and D. R. Paul, *Polymer*, 2006, **47**, 1226–1244.
29 K. A. O'Leary and D. R. Paul, *Polymer*, 2004, **45**, 6575–6585.
30 J. Fickert, C. Wohnhaas, A. Turshatov, K. Landfester and D. Crespy, *Macromolecules*, 2013, **46**, 573–579.
31 M. Barzegar-Jalali, K. Adibkia, H. Valizadeh, M. R. Siahi-Shadbad, A. Nokhodchi, Y. Omidi, G. Mohammadi, S. Hallaj-Nezhadi and M. Hasan, *J. Pharm. Pharm. Sci.*, 2008, **11**, 167–177.
32 L. S. Koester, G. G. Ortega, P. Mayorga and V. L. Bassani, *Eur. J. Pharm. Biopharm.*, 2004, **58**, 177–179.